arXiv:2412.08014v2 [cs.CV] 11 Mar 2025

MAGIC: Mastering Physical Adversarial Generation in Context through Collaborative LLM Agents

Yun Xing[1,3*], Nhat Chung[1,5*], Jie Zhang[1], Yue Cao[1,2], Ivor Tsang[1,2], Yang Liu[2], Lei Ma[3,4], Qing Guo[1†]
[1] CFAR and IHPC, Agency for Science, Technology and Research (A*STAR), Singapore
[2] Nanyang Technological University, Singapore [3] University of Alberta, Canada
[4] The University of Tokyo, Japan [5] VNU-HCM, Vietnam

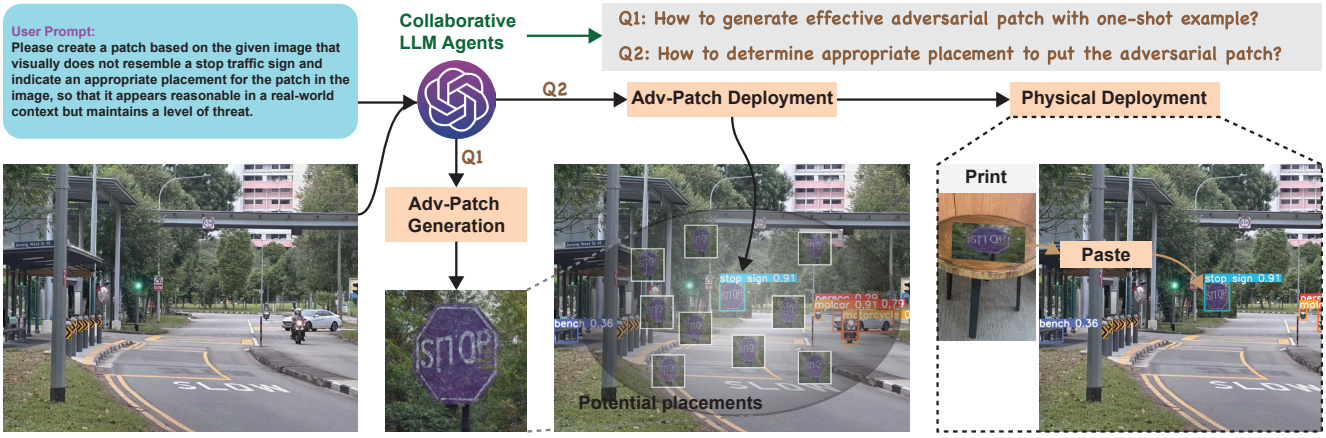


Figure 1. Intuitive idea of our proposed MAGIC framework. Given the user prompt indicates the attack subject and objective and an image of a real-world scene, our method aims to generate an attack-effective adversarial patch and automatically deploy it into the physical scene with naturalness. We propose to realize the goals through multi-modal agent planning and leverage multiple LLM-based agents to achieve collaborative generation and deployment.

Abstract

Physical adversarial attacks in driving scenarios can expose critical vulnerabilities in visual perception models. However, developing such attacks remains challenging due to diverse real-world environments and the requirement for maintaining visual naturality. Building upon this challenge, we reformulate physical adversarial attacks as a one-shot patch generation problem. Our approach generates adversarial patches through a deep generative model that considers the specific scene context, enabling direct physical deployment in matching environments. The primary challenge lies in simultaneously achieving two objectives: generating adversarial patches that effectively mislead object detection systems while determining contextually appropriate deployment within the scene. We propose MAGIC (Mastering Physical Adversarial Generation In Context), a novel framework powered by multi-modal LLM agents to address these challenges. MAGIC automatically understands scene context and generates adversarial patch through the synergistic interaction of language and vision capabilities. In particular, MAGIC orchestrates three specialized LLM agents: The adv-patch generation agent (GAgent) masters the creation of deceptive patches through strategic prompt engineering for text-to-image models. The adv-patch deployment agent (DAgent) ensures contextual coherence by determining optimal deployment strategies based on scene understanding. The self-examination agent (EAgent) completes this trilogy by providing critical oversight and iterative refinement of both processes. We validate our method on both digital and physical levels, i.e.*, nuImage and manually captured real-world scenes, where both statistical and visual results prove that our MAGIC is powerful and effective for attacking widely applied object detection systems,* i.e.*, YOLO and DETR series.*

1. Introduction

Adversarial attacks serve as a crucial method for evaluating the robustness and safety of deep learning models. Physical adversarial attacks, in particular, focus on creating adversarial patches that can be printed and deployed in the real world to mislead visual perception models [3, 15, 43, 47, 60]. Unlike their digital counterparts, physical adversarial at-

*Work done during internship at CFAR & IHPC, A*STAR. †Co-corresponding author, email address: tsingqguo@ieee.org.

tacks can directly expose vulnerabilities in deployed models during practical application [47]. This is crucial for security-sensitive applications such as autonomous driving (AD) [2, 5, 74]. When object detectors widely used in AD misidentify critical traffic participants [2, 9, 34, 42], *e.g.*, traffic signs, they may trigger incorrect vehicle responses, potentially creating hazardous situations for both drivers and pedestrians such as sudden stops on highway. By revealing these weaknesses, physical adversarial attacks underscore the need for robust perception systems in AD.

As shown in Fig. 1, physical adversarial attacks face two primary challenges: ❶ ensuring patch effectiveness against diverse real-world factors (*e.g.*, color shifts, scale variation, view angle changes), and ❷ preserving patch stealthiness within the scene, that is fooling deep models without drawing human attention. Traditionally, optimization-based adversarial patch generation methods struggle to achieve robust performance against real-world factors and state-of-the-art (SOTA) object detectors. The recent work [47] demonstrated that diffusion models can generate robust and stealthy adversarial patches via prompt engineering without optimization. However, this approach overlooks the scene context in the deployment environment, compromising both attack effectiveness and stealthiness. Specifically, [47] fails to consider three critical aspects: ❶ the influence of the deployment process on patch's attack performance, ❷ the patch's ability to remain effective and stealthy within the scene, and ❸ the suitable deployment setup of the patch within the scene. In Sec. 3, we present comprehensive analyses demonstrating that scene context and the deployment strategy significantly influence the performance of adversarial patches.

These challenges arise from the insufficient scene context understanding and the inability to integrate it into both the adversarial patch generation and deployment. A single deep model is inadequate for addressing these challenges, as scene understanding, patch generation, and deployment are distinct tasks requiring specialized capabilities. To address these challenges, we reformulate physical adversarial attacks as an one-shot patch generation problem, and develop a framework that automatically generates and deploys adversarial patches, particularly factoring in the target environment image with user-specified attack objectives. To achieve this, we propose MAGIC *(Master physical Adversarial Generation In Context through collaborative multi-modal LLM agents)*, a framework where multiple LLM agents collaboratively generate and deploy effective, stealthy adversarial patches based on comprehensive scene analyses. Our MAGIC operates in three key stages-(i) patch proposal, (ii) patch deployment, and (iii) patch refinement-powered by three specialized LLM agents (GAgent, DAgent, and EAgent) to master physical adversarial attack in real-world AD settings. In summary, our contributions are summarized as follows,

- We investigate the effectiveness of diffusion-based physical adversarial attacks [47] across diverse environments and deployment strategy, revealing that attack efficacy is highly dependent on scene context and patch deployment.
- We propose MAGIC, a novel framework that leverages collaborative multi-modal LLM agents to determine both physical adversarial patch generation and deployment based on comprehensive scene analyses. To the best of our knowledge, this is the first approach that combines LLM agents with physical adversarial generation.
- We evaluate MAGIC by attacking three well-known object detectors (YOLOv5, RT-DETR, YOLOv10) using both synthetic (*i.e.*, digital patch insertion) and physical (*i.e.*, real-world patch capturing) approaches, providing extensive analysis of their vulnerabilities in driving scenarios.

2. Related Works

Physical Adversarial Attacks. Physical adversarial attacks have been designed to stress-test perception systems used for AD in the real world [58], particularly against classification [1, 4, 11, 14, 75], detection [6, 51, 53, 65, 67, 72], and among other applications [7, 8, 10, 24, 36]. These attacks manipulate models to misclassify or overlook the targets [5], revealing practical threats to their deployment. In particular, physical adversarial patches [11, 12, 47, 62, 63, 71] are easily replicable and widely used to induce mispredictions in deployed models. Consequently, research on physical adversarial attacks, including attack effectiveness [1, 53, 63] and attack stealthiness [29, 38, 52, 57], remains essential for informing the development of safety-critical systems.

Adversarial Attack Design. Adversarial attacks exploit neural network vulnerabilities by misleading model predictions [19, 21, 23, 49, 64], which can diverge from human judgment to raise alarming safety concerns [58]. Conventionally, existing works add subtle perturbations that are not noticeable to humans [19, 21, 23], put adversarial stickers [16] or place small patches to the attack scenarios [1, 11, 26, 39, 56, 66]. Hendrycks et al. [25] found that even unedited images in the wild can pose adversarial effects. It has been hypothesized that these adversarial attacks are caused by non-robust, target-specific features that are incomprehensible to humans, rather than by inherent model issues [25, 33, 47]. Thus, a recent study [47] employs diffusion models to generate natural adversarial examples through intentional text prompt alteration to attack object detectors.

Multimodal LLM Reasoning. Inspired by the emergent capabilities of LLMs in key techniques such as zero-shot prompting [61], in-context reasoning [55], multi-modal reasoning [37, 70], and self-feedback [28], autonomous agents have made significant strides in mimicking human interactions [13, 27, 30, 41, 69, 73]. While language-based agents [48, 55] pioneered such interactions in text-based contexts, multi-modal embodied systems [27, 30, 41, 44, 69, 73] have extended these capabilities to real-world scenarios

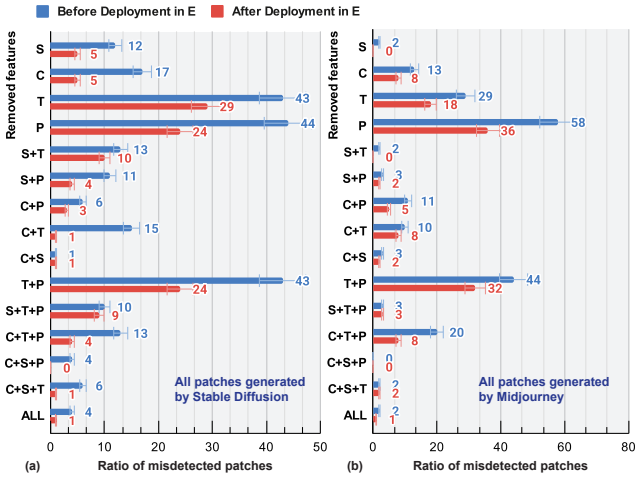


Figure 2. Detection error ratios (*i.e.*, $\epsilon_i^{\mathbb{I}}$ and $\epsilon_i^{\mathbb{I}}$) across two image sets (*i.e.* $\{\mathbb{I}_i^k\}k = 1^K$ and $\{\mathbf{I}_i^k\}k = 1^K$) for 15 prompt types ($i = 1, \ldots, 15$). The y-axis labels indicate removed features: Shape (S), Color (C), Text (T), and Pattern (P). Patch generated by (a) Stable Diffusion and (b) Midjourney.

by integrating image [18, 59, 69], video [41, 50] and audio [27]. Notably, [69] incorporated LLM reasoning for fine-grained diffusion results, demonstrating the potential of self-feedback in improving outcomes.

3. Revisit Natural Denoising Diffusion Attack

Our study is inspired by the practical obstacles encountered during real-world deployment of Natural Denoising Diffusion Attack (NDDA) [47]. Thus, we first briefly revisit NDDA then analyze the problems we encountered during the deployment which motivated us to propose the MAGIC.

3.1. Preliminaries of NDDA

NDDA leverages SOTA text-to-image (T2I) models, *e.g.*, Stable Diffusion [45], to generate physical adversarial patches through strategic manipulation of the text prompts. Given a text prompt $\mathcal{T}$ that specifies both a subject (*e.g.*, stop sign) and related robust features [20, 22] (*i.e.*, shape, color, text, and pattern), the diffusion model generates a corresponding patch. NDDA then systematically modifies the patch generation by altering the prompt $\mathcal{T}$, which selectively removes robust features from the normal stop sign. As reported in [47], the selective removal of robust features yields patches that could achieve high error detection rates while remaining stealthy to human observers. Such adversarial attack effectiveness aligns with the findings from [32], which demonstrate adversarial attacks that exploit non-robust features are predictive for DNNs but incomprehensible to humans.

3.2. NDDA in Deployment

To investigate the performance of NDDA after deployment, we set 'stop sign' as the subject and aim to generate a patch that is not stop sign but the object detector (*e.g.*, YOLOv5 [35]) can detect and misclassify it as a stop sign. Following NDDA setup, we have the benign prompt for the T2I generation, *i.e.*, 'stop sign'. We set a prompt set $\{\mathcal{T}_i\}_{i=1}^{15}$ containing 15 types of prompt where we remove different robust features from the benign stop sign. We show the 15 types in the y-axis in Fig. 2. For example, 'shape' means removing the 'shape' feature from the generated patch by setting the prompt as 'square stop sign' as the normal stop signs are an octagonal. For each prompt $\mathcal{T}_i$, we generate K patches $\{\mathbf{P}_i^k\}_{k=1}^K$ by feeding the prompt into the diffusion model and sampling K times. Here, we use the generated patches officially released by NDDA [1] to avoid any confusion.

Given an environment image $\mathbf{E}$ and a generated patch $\mathbf{P}_i^k$, we conduct two types of testing: ❶ *After deployment*. We create $\mathbf{I}_i^k$ by digitally inserting $\mathbf{P}_i^k$ at location p in the environment image with scale s representing the patch size. ❷ *Before deployment*. We also create an image $\mathbb{I}_i^k$ by inserting $\mathbf{P}_i^k$ to an empty image $\mathbf{E}^0$ with the same p and s, where $\mathbf{E}^0$ has the same size to $\mathbf{E}$ but all pixels are zero. For K patches generated from the ith prompt, we obtain $2 \times K$ images, *i.e.*, $\{\mathbf{I}_i^k\}_{k=1}^K$ and $\{\mathbb{I}_i^k\}_{k=1}^K$, and perform detection on all images using YOLOv5 [35]. For each respective set of patches, we calculate the ratio of incorrectly detected patches (*i.e.*, misdetected as stop signs) over all generated patches, denoted as $\epsilon_i^{\mathbf{I}}$ and $\epsilon_i^{\mathbb{I}}$. These metrics measure the attack effectiveness of the ith prompt both before and after the deployment.

Based on the above setups, we investigate four research questions: **RQ1:** Whether different type of patches maintain their attack effectiveness after environmental deployment? **RQ2:** How do different environments influence attack effectiveness of the generated patches? **RQ3:** How does the deployment practice influence the patches' stealthiness? **RQ4:** What is the impact of deployment location p and scale s on attack effectiveness of patches in different environments?

3.3. Empirical Results and Discussion

Response to RQ1: We investigate the influence of environment on patch attack performance by comparing detection error ratios between $\{\mathbb{I}_i^k\}_{k=1}^K$ and $\{\mathbf{I}_i^k\}_{k=1}^K$. Using the environment $\mathbf{E}_1$ shown in Fig. 3, we generate 15 paired image sets corresponding to different prompt types. For the ith paired image set, we calculate two detection error ratios: $\epsilon_i^{\mathbf{I}}$ and $\epsilon_i^{\mathbb{I}}$. The results across all 15 prompt types are presented in Fig. 2 (a), revealing several key findings: ❶ The detection error ratio before environment deployment ($\epsilon_i^{\mathbf{I}}$) generally exceeds its after-deployment counterpart ($\epsilon_i^{\mathbb{I}}$) across all prompt types, demonstrating that environment deployment significantly degraded the patches' performance. ❷ The magnitude of reduction in detection error ratios varies notably across prompt types, indicating that text prompts have influence on the environment deployment. ❸ The pattern of detection error ratios across prompts remains consistent between Stable Diffusion and Midjourney generations when comparing

[1] https://sites.google.com/view/av-ioat-sec/ndd-attack

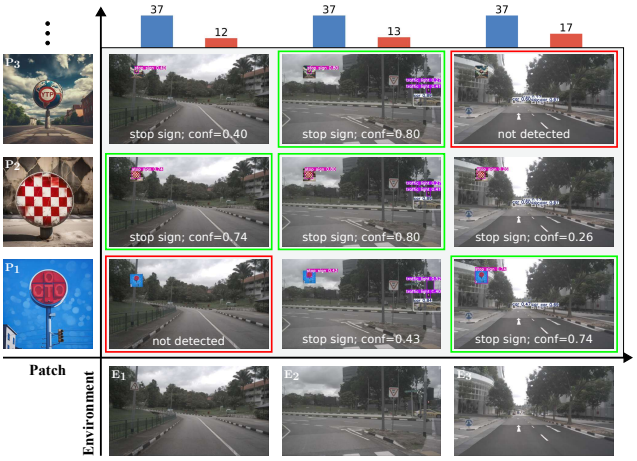


Figure 3. Visualization of three generated patches ($\mathbf{P}_1$,$\mathbf{P}_2$,$\mathbf{P}_3$), three environments ($\mathbf{E}_1$,$\mathbf{E}_2$,$\mathbf{E}_3$), and the detection results with YOLOv5 across them. The confidence score (conf.) > 0.5 means the patch realizes the attack goal. Bar plot at the top: detection error ratios before (blur) and after (red) deployment over all the NDDA patches for each of the environments.

Fig. 2 (b) with Fig. 2 (a), suggesting these findings generalize across different image generation architectures.

Response to RQ2: We deploy generated patches into different environments to see whether environments would affect the attack effectiveness. As shown in Fig. 3, we paste three generated non-stop sign patches $\{\mathbf{P}_i\}_{i=1}^3$ into three different environments $\{\mathbf{E}_i\}_{i=1}^3$ at the same location with the same scale. Meanwhile, following the setups in the response to RQ1, we calculate the detection error ratios before deployment and after deployment for all the generated patches. We observe that the same patch presents different attack effectiveness in different environments. For example, $\mathbf{P}_3$ could be identified as stop sign in the $\mathbf{E}_2$ with a high confidence 0.80, while it is missed in $\mathbf{E}_3$. The same detection error ratios can be derived across all different environments.

Response to RQ3: For practical viability and ensuring human observers will not be distracted by the patch, the deployment of the generated patch should be physically feasible and contextually plausible. As illustrated in Fig. 3, the patches' location in $\mathbf{E}_1$ appears natural as advertising boards, maintaining environmental coherence. In contrast, patches in $\mathbf{E}_2$ are positioned in the sky, violating physical constraints, while those in $\mathbf{E}_3$ are placed on the building facade, creating contextually incongruous arrangements.

Response to RQ4: We divide the scene image into a 3×3 grid of regions and designate each region's center as a location for patch insertion, testing four different patch scales (See Fig. 4 (a)-(b)). We evaluate the detection confidence of the stop sign across all patch deployments in each environment and visualize the results using radar maps. As illustrated in Fig. 4 (c)-(f), we observe two key patterns: ❶ for large-scale patches (s_3 and s_4), the detection confidence remains relatively consistent across different locations; ❷ for small-scale patches (s_1 and s_2), the detection confidence varies substantially across locations, with distinct patterns emerging across different patches and environments.

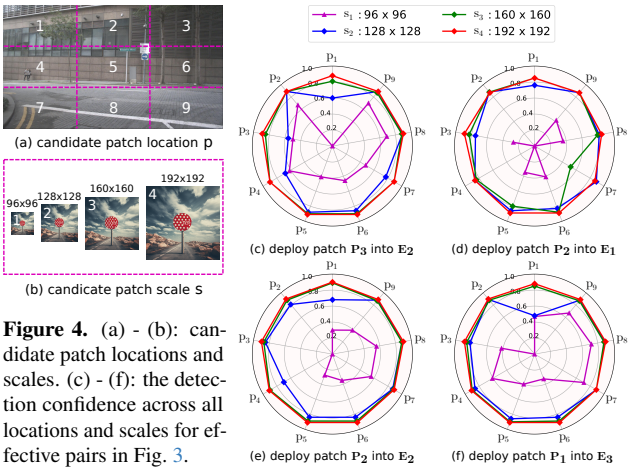


Figure 4. (a) - (b): candidate patch locations and scales. (c) - (f): the detection confidence across all locations and scales for effective pairs in Fig. 3.

Motivations. From the above analysis, we see environments cast great influence on the patches' performance, where different environments require unique deployment strategy. Obviously, a novel physical adversarial patch attack framework is needed to ❶ generate environment-oriented adversarial patch for various real-world environments, ❷ determine contextually appropriate deployment for the generated patch within a given scene, and ❸ keep misleading object detection systems after deployment. In this work, we propose the MAGIC framework which formulates the problem as an one-shot patch generation task and orchestrates three specialized LLM agents to realize these objectives.

4. MAGIC Methodology

4.1. Overview

We propose using a multi-modal LLM denoted as $\mathcal{V}$ to handle the three distinct requirements by iteratively refining the adversarial patch generation and deployment. (See Fig. 5) Given the initial user prompt $\mathcal{T}$ indicating the attack subject and objective, we first build the adv-patch generation agent (GAgent, *i.e.*, $\mathcal{V}_\text{G}$) that predicts a text prompt based on the $\mathcal{T}$ which feed into the T2I diffusion model to generate an adversarial patch. The process is formulated as,

$$\mathbf{P}_i = \mathcal{V}_\text{G}(\mathcal{T}_i, \mathcal{G}(\cdot), \mathcal{X}_\text{G}), \tag{1}$$

where $\mathcal{T}_i$ is the attack subject and objective at the ith iteration. We have $\mathcal{T}_0 = \mathcal{T}$, $\mathcal{G}(\cdot)$ is the T2I diffusion model to generate the adversarial patch according to the text prompt, and $\mathcal{X}_\text{G}$ is the instruction defining $\mathcal{V}_\text{G}$'s capability. To allow the refinement, we update $\mathcal{T}_i$ according to the final result of iteration $i-1$. Please refer to Sec. 4.2 for details.

With the generated adv-patch $\mathbf{P}_i$, we setup the adv-patch deployment agent (DAgent, *i.e.*, $\mathcal{V}_\text{D}$) empowered with set-of-mark (SoM) [68] to determine its appropriate location p_i and scale s_i within the image $\mathbf{E}$ of target environment.

$$(p_i, s_i) = \mathcal{V}_\text{D}(\mathbf{E}, \mathbf{P}_i, \mathcal{S}(\cdot), \mathcal{X}_\text{D}), \tag{2}$$

where the instruction $\mathcal{X}_\text{D}$ defines $\mathcal{V}_\text{D}$'s capability and $\mathcal{S}(\cdot)$ is the SoM prompting. DAgent's processing details are

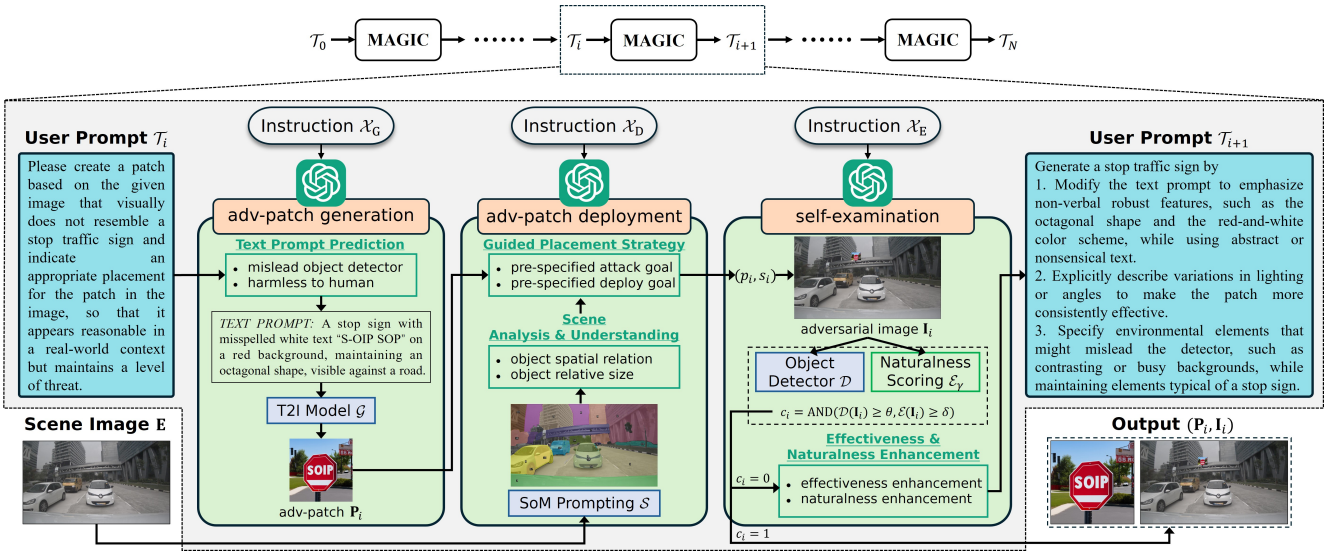


Figure 5. Overall pipeline of the proposed MAGIC framework. Please zoom in for better visualization.

presented in Sec. 4.3. Subsequently, we insert the patch $\mathbf{P}_i$ into $\mathbf{E}$ at p_i with scale s_i getting the adversarial image $\mathbf{I}_i$.

However, we do not know whether the adversarial image is good enough to mislead the object detector $\mathcal{D}(\cdot)$ and meet the requirement of scene coherence or not. To address this issue, we propose to build a self-examination agent (EAgent, *i.e.*, $\mathcal{V}_\text{E}$) that can analyze the adversarial image $\mathbf{I}_i$ and optimize the user prompt $\mathcal{T}_{i+1}$. We formulate the process as,

$$(\mathcal{T}_{i+1}, c_i) = \mathcal{V}_\text{E}(\mathbf{I}_i, \mathcal{T}_i, \mathcal{D}(\cdot), \mathcal{X}_\text{E}), \tag{3}$$

where the instruction $\mathcal{X}_\text{E}$ defines $\mathcal{V}_\text{E}$'s capability and c_i is a binary examination result. If $c_i = 0$, we trigger the next round iteration by setting $i = i + 1$, otherwise, we stop iteration and output $\mathbf{P}_i$ and $\mathbf{I}_i$ as the final result. We explain the details of EAgent at Sec. 4.4.

4.2. Adv-Patch Generation Agent (GAgent)

At the ith iteration, we have the user prompt $\mathcal{T}_i$ and the input environment image $\mathbf{E}$. We first prompt the LLM $\mathcal{V}$ with the instruction $\mathcal{X}_\text{G}$ to predict a text prompt $\mathcal{P}_i$, which describes the patch we want to generate, based on the user prompt $\mathcal{T}_i$. Then, we feed the text prompt into $\mathcal{G}$, *i.e.*, Stable Diffusion v2 [45], and obtain an adversarial patch $\mathbf{P}_i = \mathcal{G}(\mathcal{P}_i)$. Note that the text prompt prediction capability of $\mathcal{V}$ is defined by the instruction $\mathcal{X}_\text{G}$ as detailed in the following.

Instruction: $\mathcal{X}_\text{G}$

I will show you with a user prompt which described the subject and objective of a visual patch. You are required to predict a text description of the subject that can potentially achieve the specified objectives. The ultimate goal is to let the visual patch generated based on the text description has a deceptive appearance, such that
- an object detector will recognize the visual patch as an instance of a specific semantic category with high confidence,
- but human observers will recognize the visual patch as just an abstract art which does not belongs to any specific category.

4.3. Adv-Patch Deployment Agent (DAgent)

With the generated patch $\mathbf{P}_i$, we aim to determine its appropriate deployment location p_i and scale s_i for the given environmental image $\mathbf{E}$. To achieve this, SoM prompting $\mathcal{S}$ [68] is firstly applied to tag the key elements within $\mathbf{E}$. Then we prompt the LLM $\mathcal{V}$ with instruction $\mathcal{X}_\text{D}$ to comprehend SoM results and determine the most potential location and scale within the $\mathbf{E}$ that can achieve the objectives specified by $\mathcal{T}_i$. The instruction $\mathcal{X}_\text{D}$ is detailed in the below.

Instruction: $\mathcal{X}_\text{D}$

You are provided with an image of a scene and the corresponding semantic segmentation results marked with numbers. For a given visual patch, you are required to accomplish the following two tasks:
1. **Scene Analysis & Understanding: a.** Perceive all the elements within the given environment image. **b.** Comprehend the spatial relationship and relative size of all the elements inside the scene by referring to the numbered segmentations.
2. **Guided Placement Strategy: a.** Check the content of the given patch and compare it with the elements in the environment. **b.** Comprehend the pre-defined attack effectiveness and deployment stealthiness goal. (See supplemental material for details) **c.** Based on the patch content, determine where should the patch be placed so that the goals can be achieved. **d.** Based on the determined patch location, decide what scale should be applied to the patch so that the goals can be achieved.

Once the deployment location p_i and scale s_i are determined, we resize the patch $\mathbf{P}_i$ to s_i and place it at p_i in the scene image $\mathbf{E}$, which results the adversarial image $\mathbf{I}_i$.

4.4. Self-Examination Agent (EAgent)

With the adversarial image ready, we proceed to assess the patch's performance for attacking the object detector and keeping stealthy within the scene. We first feed $\mathbf{I}_i$ into the target object detector $\mathcal{D}$ to get detection results $\hat{\mathbf{I}}_i = \mathcal{D}(\mathbf{I}_i)$. Then we inspect if the detection confidence of the patch passes the pre-defined threshold θ as $\mathcal{D}(\mathbf{I}_i) \geq \theta$. Then $\mathbf{P}_i$ is recognized as attack effective if the inequality holds true.

To determine the patch's naturalness, we prompt an in-

dependent LLM $\mathcal{E}$ with instruction γ to generate a naturalness score for the patch. Similarly, we set a naturalness threshold δ and check whether the generated patch satisfies $\mathcal{E}(\mathbf{I}_i, \gamma) \geq \delta$. The patch $\mathbf{P}_i$ is then deemed as natural if this inequality holds true. We detail the instruction γ as follows:

Naturalness Score Instruction: γ

You are provided with an image of a visual patch and an image where the patch is deployed into an environment. Supposing you are a human observer, you are required to judge whether the patch is natural or not within the environment with regarding to its location and scale.

1. **Image Understanding:** Perceive all the elements inside the given image in respect of their spatial relation and relative size.
2. **Location Inspection:** Check the patch's location within the image and determine whether it is a reasonable place for placing the patch.
3. **Scale Inspection:** Check the patch's scale and determine whether its size is reasonable compared to other objects inside the image.
4. **Naturalness Summarization:** Give a score range from 0 to 1 by aggregating the above reasoning of the patch's location and scale.

Afterwards, we set c_i as a binary operator, calculated by $c_i = \text{AND}(\mathcal{D}(\mathbf{I}_i) \geq \theta, \mathcal{E}(\mathbf{I}_i, \gamma) \geq \delta)$, to get the final examination results. If $c_i = 1$, the iteration is exited and $(\mathbf{P}_i, \mathbf{I}_i)$ is returned. Otherwise, refinement is required and we further prompt the LLM $\mathcal{V}$ with instruction $\mathcal{X}_\text{E}$ to update the user prompt $\mathcal{T}_i$ based on the assessment results. Then a new round of agent planning is started by setting $\mathcal{T}_i = \mathcal{T}_{i+1}$.

Instruction: $\mathcal{X}_\text{E}$

You are provided with an image where a visual patch is deployed into an environment. The image has been evaluated for its effectiveness of attacking the target object detector and the naturalness within the environment. Given the evaluation results, you are required to reflect on why the patch can or cannot be effective or natural then propose suggestions of how to change the patch's appearance.

1. **Attack Rules Understanding:** Comprehend the pre-defined rules of how to attack an object detector by deploying a visual patch within a scene. (See supplemental material for the definition of rules)
2. **Attack Effectiveness Enhancement: a.** Perceive the patch's appearance in the image and summarize the detection result. **b.** Compare the patch in the image to the rules then summarize your understanding of why the patch is not attack effective.
3. **Deployment Naturalness Enhancement: a.** Perceive the patch's location and scale in the image and summarize the naturalness evaluation results. **b.** Compare the patch in the image to the rules then suggest how to adjust its location and scale to make it more natural.

4.5. Extension to Physical World

Finally, we get the optimal patch $\mathbf{P}^*$ and the corresponding deployment strategy (p^*, s^*). Then, we physically deploy the patch $\mathbf{P}^*$ by printing it out, place it at the location p^* in $\mathbf{E}$ and re-capture an image of the scene with the patch size as s^* to match the reference image $\mathbf{I}$. While our MAGIC provides the optimal patch location and scale, other real-world factors, like printing color shift and viewing angle, are also well-known to deteriorate the digital-to-physical (D2P) transferability. In fact, our MAGIC prioritizes robust features that maintain the patch performance adaptively during the generation and deployment, minimizing the D2P degradation. We show evidence that MAGIC is robust to both viewing angle and printing color shift in supplemental material.

5. Experiments

5.1. Experimental Setup

Digital & Physical Environments. We adopt the images from nuImage [17] for digital evaluation, which consists of images captured by 6 car-mounting cameras from different view, *i.e.*, back, back left, back right, front, front left, front right. We select one image for each view (Fig. 6) as an initial study. We further physically verify our MAGIC framework with two different physical scenarios (Fig. 7). One is a real-world busy bus stop scene and another is a regular road next to a college with few pedestrians. More physical experiments can be found in supplemental materials.

Baselines. As NDDA [47] is the very initial study of natural denoising diffusion attacking, we validate our method by setting NDDA as the baseline. In specific, we combine NDDA with two different deployment strategies as the baselines. ❶ We first deploy the patches from NDDA with random location, dubbed "NDDA Rand", which can be utilized to verify the deployment ability of our MAGIC. ❷ For the second baseline, we keep using the patches from NDDA but adopt our DAgent as the deployment strategy, named "NDDA+DAgent" which can effectively demonstrate the advantage of our MAGIC in generating effective patches.

Generator & Detectors. To keep the fairness of comparison, we follow NDDA and adopt Stable Diffusion v2 [46] as the generator. For target detectors, the commonly used YOLOv5 [35] and RT-DETR [40] are tested. Moreover, we empirically found that YOLOv5 and DETR are out-of-date and easily to be disturbed, thus we further adopt YOLOv10 [54] as our main evaluation target. For all three detectors, we use the API from ultralytics to keep the consistency.

Metrics. We evaluate the patches' attack performance by Attack Success Rate (ASR), which measures the percentage of the patches that successfully deceived the target object detector. ASR has a range from 0 to 100, where higher values signifying greater adversarial attack performance.

5.2. Digital Comparative Results

Attack Effectiveness. There are 50 patches for each text prompt (refer to Sec. 3.2) in NDDA. And there are several text prompts removed the same robust feature, *e.g.*, both 'square_stop_sign' and 'triangle_stop_sign'. For comparison fairness, we generate the same number of patches for a given environment and report the average results over all the patches of the same text prompt type in NDDA. Note that for the NDDA+DAGent baseline, we setup two variants, *i.e.*, text removed and pattern removed, as we empirically found they are more effective than other type of text prompt.

Results. Following NDDA setup, we first evaluate the patches with a confidence threshold of 0.5. The statistical results are tabulated in Tab. 1. ❶ Comparing to the baselines, we see our MAGIC enjoys a great attack effectiveness

Table 1. Comparative ASR results by evaluating our MAGIC and NDDA patches with different detectors for nuImage environments. The confidence threshold is set to 0.5 as the same of NDDA. The best results are highlighted in red and the second best in blue, while the best results of each detector for a given environment are marked as **bold** and the second best as *italic*.

		Removed Robust Features				Object Detectors			
		Shape	Color	Text	Pattern	YOLOv5	RT-DETR	YOLOv10	Avg.
Environment ①	NDDA Rand	✔				23.00%	23.00%	10.00%	18.66%
			✔			15.00%	48.00%	6.00%	23.00%
				✔		46.00%	56.00%	30.00%	44.00%
					✔	47.00%	56.00%	32.00%	45.00%
		✔	✔	✔	✔	8.66%	9.33%	4.66%	7.55%
	NDDA+DAgent			✔		*48.00%*	51.00%	33.00%	44.00%
	NDDA+DAgent				✔	47.00%	*57.00%*	*36.00%*	46.66%
	MAGIC (ours)					**88.00%**	**80.00%**	**74.00%**	80.66%
Environment ②	NDDA Rand	✔				14.00%	40.00%	17.00%	23.66%
			✔			9.00%	51.00%	10.00%	23.33%
				✔		42.00%	74.00%	32.66%	49.55%
					✔	41.00%	71.00%	36.00%	49.33%
		✔	✔	✔	✔	6.00%	21.00%	4.00%	10.33%
	NDDA+DAgent			✔		45.00%	*78.00%*	36.00%	53.00%
	NDDA+DAgent				✔	*51.00%*	78.00%	*39.33%*	56.11%
	MAGIC (ours)					**66.00%**	**94.00%**	**92.00%**	84.00%
Environment ③	NDDA Rand	✔				15.00%	21.00%	6.00%	14.00%
			✔			5.00%	39.00%	11.00%	18.33%
				✔		40.00%	58.00%	26.66%	41.55%
					✔	38.00%	59.00%	3.00%	33.33%
		✔	✔	✔	✔	2.00%	12.00%	2.00%	4.66%
	NDDA+DAgent			✔		*43.00%*	*60.00%*	*33.00%*	45.33%
	NDDA+DAgent				✔	*43.00%*	*60.00%*	28.00%	43.66%
	MAGIC (ours)					**84.00%**	**94.00%**	**90.00%**	89.33%
Environment ④	NDDA Rand	✔				16.00%	14.00%	7.00%	12.33%
			✔			10.00%	33.00%	6.00%	16.33%
				✔		42.66%	53.33%	23.33%	39.77%
					✔	45.00%	47.00%	28.00%	40.00%
		✔	✔	✔	✔	4.66%	10.00%	1.33%	5.33%
	NDDA+DAgent			✔		43.00%	*58.00%*	*32.00%*	44.33%
	NDDA+DAgent				✔	*49.00%*	49.00%	*32.00%*	43.33%
	MAGIC (ours)					**78.00%**	**90.00%**	**80.00%**	82.66%
Environment ⑤	NDDA Rand	✔				13.00%	30.00%	6.00%	16.33%
			✔			10.00%	49.00%	9.00%	22.66%
				✔		44.66%	72.66%	32.00%	49.77%
					✔	49.00%	67.00%	36.00%	50.66%
		✔	✔	✔	✔	7.33%	19.33%	2.66%	9.77%
	NDDA+DAgent			✔		49.00%	*71.00%*	39.00%	53.00%
	NDDA+DAgent				✔	*51.00%*	71.00%	*40.00%*	54.00%
	MAGIC (ours)					**72.00%**	**92.00%**	**74.00%**	79.33%
Environment ⑥	NDDA Rand	✔				14.00%	27.00%	10.00%	17.00%
			✔			8.00%	49.00%	10.00%	22.33%
				✔		39.33%	60.00%	25.33%	41.55%
					✔	43.00%	57.00%	28.00%	42.66%
		✔	✔	✔	✔	3.33%	12.00%	2.66%	5.99%
	NDDA+DAgent			✔		42.00%	*66.00%*	*32.00%*	46.66%
	NDDA+DAgent				✔	*45.00%*	60.00%	*32.00%*	45.66%
	MAGIC (ours)					**92.00%**	**96.00%**	**84.00%**	90.66%

boosting for all the environments. Such cross-environment superior ASR performance verified the effective patch generation capability of our MAGIC. ❷ While the NDDA Rand only achieves random attacking, *i.e.*, around 50%, under the best robust feature removing setup, we observe that they still receive great boosting with our DAgent proving it can facilitates the attack by placing the patch more reasonably.

We further evaluate the attack performance of our MAGIC patches with a 0.8 confidence threshold in Tab. 2. With such a high threshold, we aim to push our MAGIC to a random attacking state for determining its maximum capability. ❶ We first observe that our MAGIC maintains its performance across detectors with such a high detection threshold, where the average ASR 58.66% is even competitive comparing with the NDDA performance with 0.5 threshold. Such phenomenon strongly demonstrates our MAGIC possesses powerful attack capabilities. ❷ Another phenomenon worth to be mentioned is that the DAgent fails to improve NDDA under 0.8 threshold, which is contradict to what we conclude when the threshold is set to 0.5. We note such results are expected since DAgent is mainly designed to improve the

Table 2. Comparing the statistical ASR results with different confidence threshold, *i.e.*, 0.5 *v.s.* 0.8, by evaluating the the patch generated by our MAGIC and NDDA with different detectors in Environment ①. The best average results are highlighted in red, while the second best in blue, and the best results for each detector are marked as **bold**.

		Removed Robust Features				Object Detectors			
		Shape	Color	Text	Pattern	YOLOv5	RT-DETR	YOLOv10	Avg.
threshold *0.5*	NDDA Rand	✔				23.00%	23.00%	10.00%	18.66%
			✔			15.00%	48.00%	6.00%	23.00%
				✔		46.00%	56.00%	30.00%	44.00%
					✔	47.00%	56.00%	32.00%	45.00%
		✔	✔	✔	✔	8.66%	9.33%	4.66%	7.55%
	NDDA+DAgent			✔		48.00%	51.00%	33.00%	44.00%
	NDDA+DAgent				✔	47.00%	57.00%	36.00%	46.66%
	MAGIC (ours)					**88.00%**	**80.00%**	**74.00%**	80.66%
threshold *0.8*	NDDA Rand	✔				6.00%	9.00%	3.00%	6.00%
			✔			7.00%	25.00%	5.00%	12.33%
				✔		30.00%	37.33%	20.00%	29.11%
					✔	25.00%	34.00%	25.00%	28.00%
		✔	✔	✔	✔	2.66%	4.66%	3.00%	2.44%
	NDDA+DAgent			✔		25.33%	32.00%	20.00%	25.77%
	NDDA+DAgent				✔	23.33%	30.00%	25.33%	26.22%
	MAGIC (ours)					**56.00%**	**74.00%**	**46.00%**	58.66%



Figure 6. Illustration of the patch deployment results for NDDA baselines and our MAGIC framework in different environments. Patches are pointed out with red arrows. Please zoom in for better visualization.

stealthiness rather than boost the attack effectiveness.

Deployment Naturality. We randomly sample patches from NDDA dataset for comparing the deployment naturalness, and the patches adopted for our MAGIC are generated through the pipeline. Note that a better placement means the patch is more easy for physical deployment implementation and more natural to human observers. We also reported the statistical results, please find them in supplemental material.

Results. As shown in Fig. 6, we visually compare the patch deployment results of our MAGIC and baselines over the selected 6 environments. ❶ Comparing the placement of NDDA Rand against the placement planned by our DAgent in NDDA+DAgent, we see clearly that our DAgent is able to place the patch in a more appropriate location in the scene where the patch is more practical for deployment. ❷ Furthermore, it can be observed that the digital-level deployment results of our MAGIC patches are visually better consistent within the given scene when compared with NDDA+DAgent. This is because our MAGIC considered contextually consistency of the patches during the patch deployment process.

5.3. Physical Comparative Results

We test in two physical environments (see Fig. 7): ❶ one is a bus stop bay with heavy traffics; ❷ one is a regular road next

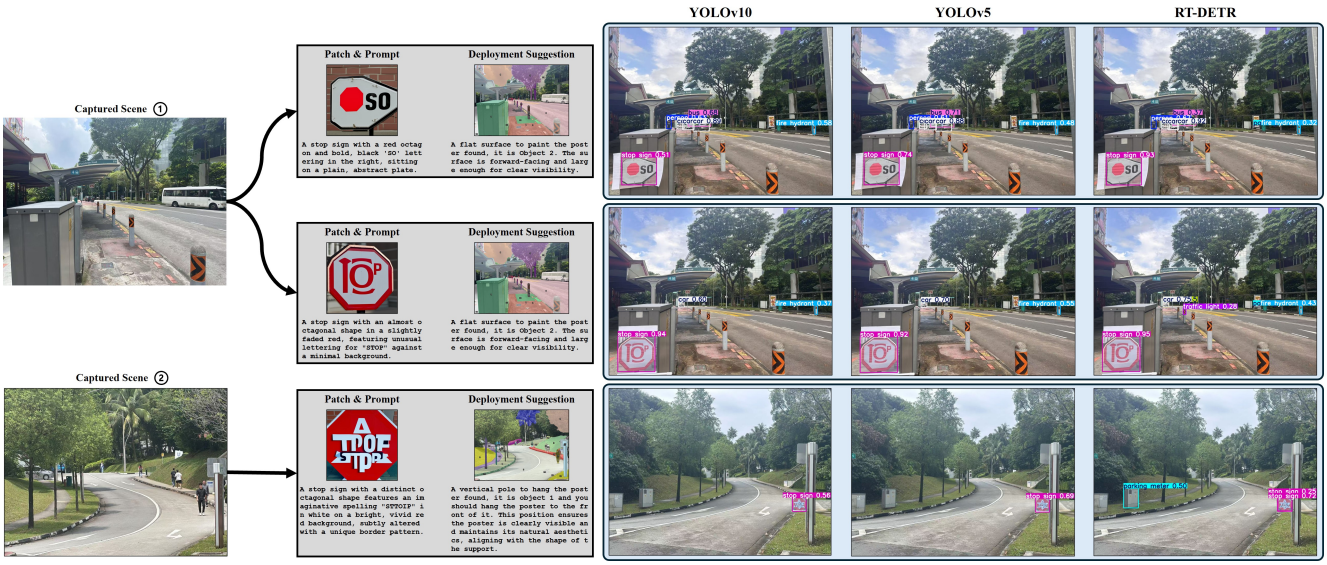


Figure 7. Illustration of the physical attack cases generated by the proposed MAGIC and the corresponding object detection results.

to a college with some pedestrians on the sidewalk. In order to verify the flexibility of our MAGIC, we select the bus stop scene and generate two patches for it. **We also provided video results and more visualizations within various real-world scenes. Note that we ensured the patches were not observed by vehicles on the road and discussed ethical issues. Please find all of them in supplemental material.**

Results. As visualized in Fig. 7, we show the generated patch with prompt, the deployment suggestion and the detection results. ❶ First, observing the generally lower detection confidences, we see that the physical attacks are more harder to realize due to the environment variance. Even so, our MAGIC still generates an extremely effective attack patch, *i.e.*, the second patch for scene ①. ❷ Second, comparing the detection results of the three detectors, we observe that YOLOv5 and RT-DETR are more prone being attacked while YOLOv10 is more robust to the attacks. However, all the generated patches are proven to be physically attack effective for YOLOv10 which further verified the physical effectiveness of our MAGIC. ❸ Third, by comparing the two scenes' results, we see that our MAGIC is capable of giving out contextually appropriate patch and location for real-world deployment. In summary, we can conclude from the results that our MAGIC is full of power for attacking the object detection system in the real-world scenarios.

6. Ablation Study

❶ We start from the basic patch generation function of our framework, where GAgent is isolated without either deployment or self-examination and is denoted as "GAgent-*naïve*". ❷ The further functionality that our MAGIC provided is the contextually appropriate deployment of DAgent. Thus, we combine GAgent with the patch deployment planning as the second ablation, denoted as "GAgent-*naïve w/* DAgent". ❸ Then, we note that the EAgent is responsible for supervising both patch attack effectiveness (ae) and deployment naturality (dn), so we combine GAgent with the patch attack supervision of EAgent which denotes as "GAgent-*naïve w/* EAgent-ae". Finally, we involve the deploy naturality of EAgent getting the proposed MAGIC framework.

Results. As tabulated in Tab. 3, we see that naive patch generation without any text prompt engineering cannot attack the detectors at all. Consequently, it is obvious that the DAgent cannot significantly contribute to the improvement of the attack performance for GAgent, *i.e.*, GAgent-*naïve w/* DAgent. On the contrary, the involvement of attack effectiveness supervision from EAgent greatly boosted the attack effectiveness of the generated patch against all detectors, achieving 39.67%, 45.00% attack effectiveness improvements compared to the DAgent baseline. Finally, our MAGIC achieves its best attack performance by benefiting to the supervision of EAgent and also the appropriate deployment of DAgent.

Table 3. Bblation results of the proposed MAGIC with two different environment image. The best average results are highlighted in red, while the best results for each detector and environment are marked in **bold**.

		Object Detectors			
	Model	YOLOv5	RT-DETR	YOLOv10	Avg.
Env. ①	GAgent-*naïve*	4.00%	6.00%	0%	3.33%
	GAgent-*naïve w/* DAgent	7.00%	9.00%	0%	5.33%
	GAgent-*naïve w/* EAgent-ae	46.00%	56.00%	33.00%	45.00%
	MAGIC	**88.00%**	**80.00%**	**74.00%**	80.66%
Env. ②	GAgent-*naïve*	2.00%	2.00%	0%	1.33%
	GAgent-*naïve w/* DAgent	6.00%	6.00%	3.00%	5.00%
	GAgent-*naïve w/* EAgent-ae	23.00%	60.00%	67.00%	50.00%
	MAGIC	**66.00%**	**94.00%**	**92.00%**	84.00%

7. Conclusion

In this work, we propose the MAGIC framework which reformulates physical adversarial attacks as an one-shot patch generation problem. Our approach generates adversarial patches that considered the influence of scene context, enabling direct physical deployment in matching environments.

By conducting experiments on both digital and physical levels, we demonstrate that our method can effectively generate context-aware patch, deploy the patch in real world and attack widely applied object detectors. To the best of our knowledge, our work is the very initial study to improve and extend the natural diffusion attack in physical scenarios.

References

[1] Tom B Brown, Dandelion Mané, Aurko Roy, Martín Abadi, and Justin Gilmer. Adversarial patch. In *Proceedings of the Advances in Neural Information Processing Systems Workshop*, 2017. 2

[2] Holger Caesar, Varun Bankiti, Alex H. Lang, Sourabh Vora, Venice Erin Liong, Qiang Xu, Anush Krishnan, Yu Pan, Giancarlo Baldan, and Oscar Beijbom. nuscenes: A multimodal dataset for autonomous driving. In *2020 IEEE/CVF Conference on Computer Vision and Pattern Recognition*, 2020. 2

[3] Yue Cao, Yun Xing, Jie Zhang, Di Lin, Tianwei Zhang, Ivor Tsang, Yang Liu, and Qing Guo. Scenetap: Scene-coherent typographic adversarial planner against vision-language models in real-world environments. *arXiv preprint arXiv:2412.00114*, 2024. 1

[4] Stephen Casper, Max Nadeau, Dylan Hadfield-Menell, and Gabriel Kreiman. Robust feature-level adversaries are interpretability tools. *Advances in Neural Information Processing Systems*, 35:33093–33106, 2022. 2

[5] Li Chen, Penghao Wu, Kashyap Chitta, Bernhard Jaeger, Andreas Geiger, and Hongyang Li. End-to-end autonomous driving: Challenges and frontiers. *IEEE Transactions on Pattern Analysis and Machine Intelligence*, 46(12):10164–10183, 2024. 2

[6] Shang-Tse Chen, Cory Cornelius, Jason Martin, and Duen Horng Polo Chau. Shapeshifter: Robust physical adversarial attack on faster r-cnn object detector. In *Joint European Conference on Machine Learning and Knowledge Discovery in Databases*, pages 52–68. Springer, 2018. 2

[7] Zhiyuan Cheng, James Liang, Hongjun Choi, Guanhong Tao, Zhiwen Cao, Dongfang Liu, and Xiangyu Zhang. Physical attack on monocular depth estimation with optimal adversarial patches. In *ECCV*, pages 514–532. Springer, 2022. 2

[8] Nhat Chung, Sensen Gao, Tuan-Anh Vu, Jie Zhang, Aishan Liu, Yun Lin, Jin Song Dong, and Qing Guo. Towards transferable attacks against vision-llms in autonomous driving with typography. *arXiv preprint arXiv:2405.14169*, 2024. 2

[9] Thierry Deruyttere, Simon Vandenhende, Dusan Grujicic, Luc Van Gool, and Marie Francine Moens. Talk2car: Taking control of your self-driving car. In *Proceedings of the 2019 Conference on Empirical Methods in Natural Language Processing and the 9th International Joint Conference on Natural Language Processing (EMNLP-IJCNLP)*, pages 2088–2098, 2019. 2

[10] Li Ding, Yongwei Wang, Kaiwen Yuan, Minyang Jiang, Ping Wang, Hua Huang, and Z Jane Wang. Towards universal physical attacks on single object tracking. In *Proceedings of the AAAI Conference on Artificial Intelligence*, pages 1236–1245, 2021. 2

[11] Bao Gia Doan, Minhui Xue, Shiqing Ma, Ehsan Abbasnejad, and Damith C Ranasinghe. Tnt attacks! universal naturalistic adversarial patches against deep neural network systems. *IEEE Transactions on Information Forensics and Security*, 17:3816–3830, 2022. 2

[12] Andrew Du, Bo Chen, Tat-Jun Chin, Yee Wei Law, Michele Sasdelli, Ramesh Rajasegaran, and Dillon Campbell. Physical adversarial attacks on an aerial imagery object detector. In *Proceedings of the IEEE/CVF Winter Conference on Applications of Computer Vision*, pages 1796–1806, 2022. 2

[13] Yilun Du, Shuang Li, Antonio Torralba, Joshua B. Tenenbaum, and Igor Mordatch. Improving factuality and reasoning in language models through multiagent debate. In *Forty-first International Conference on Machine Learning*, 2024. 2

[14] Kevin Eykholt, Ivan Evtimov, Earlence Fernandes, Bo Li, Amir Rahmati, Chaowei Xiao, Atul Prakash, Tadayoshi Kohno, and Dawn Song. Robust physical-world attacks on deep learning visual classification. In *CVPR*, pages 1625–1634, 2018. 2

[15] Kevin Eykholt, Ivan Evtimov, Earlence Fernandes, Bo Li, Amir Rahmati, Chaowei Xiao, Atul Prakash, Tadayoshi Kohno, and Dawn Song. Robust physical-world attacks on deep learning visual classification. In *2018 IEEE Conference on Computer Vision and Pattern Recognition*, pages 1625–1634. Computer Vision Foundation / IEEE Computer Society, 2018. 1

[16] Kevin Eykholt, Ivan Evtimov, Earlence Fernandes, Bo Li, Amir Rahmati, Chaowei Xiao, Atul Prakash, Tadayoshi Kohno, and Dawn Song. Robust physical-world attacks on deep learning visual classification. In *2018 IEEE Conference on Computer Vision and Pattern Recognition*, pages 1625–1634, 2018. 2

[17] Whye Kit Fong, Rohit Mohan, Juana Valeria Hurtado, Lubing Zhou, Holger Caesar, Oscar Beijbom, and Abhinav Valada. Panoptic nuscenes: A large-scale benchmark for lidar panoptic segmentation and tracking. *arXiv preprint arXiv:2109.03805*, 2021. 6

[18] Xingyu Fu, Yushi Hu, Bangzheng Li, Yu Feng, Haoyu Wang, Xudong Lin, Dan Roth, Noah A. Smith, Wei-Chiu Ma, and Ranjay Krishna. BLINK: multimodal large language models can see but not perceive. *CoRR*, abs/2404.12390, 2024. 3

[19] Sensen Gao, Xiaojun Jia, Xuhong Ren, Ivor W. Tsang, and Qing Guo. Boosting transferability in vision-language attacks via diversification along the intersection region of adversarial trajectory. In *Computer Vision - ECCV 2024*, pages 442–460, 2024. 2

[20] Yunhao Ge, Yao Xiao, Zhi Xu, Xingrui Wang, and Laurent Itti. Contributions of shape, texture, and color in visual recognition. In *European Conference on Computer Vision*, pages 369–386. Springer, 2022. 3

[21] Ian J. Goodfellow, Jonathon Shlens, and Christian Szegedy. Explaining and harnessing adversarial examples. In *3rd International Conference on Learning Representations*, 2015. 2

[22] Kalanit Grill-Spector and Rafael Malach. The human visual cortex. *Annu. Rev. Neurosci.*, 27(1):649–677, 2004. 3

[23] Jindong Gu, Hengshuang Zhao, Volker Tresp, and Philip H. S. Torr. Segpgd: An effective and efficient adversarial

attack for evaluating and boosting segmentation robustness. In *Computer Vision - ECCV*, pages 308–325, 2022. 2

[24] Qing Guo, Xiaofei Xie, Felix Juefei-Xu, Lei Ma, Zhongguo Li, Wanli Xue, Wei Feng, and Yang Liu. Spark: Spatial-aware online incremental attack against visual tracking. In *European conference on computer vision*, pages 202–219. Springer, 2020. 2

[25] Dan Hendrycks, Kevin Zhao, Steven Basart, Jacob Steinhardt, and Dawn Song. Natural adversarial examples. In *IEEE Conference on Computer Vision and Pattern Recognition*, pages 15262–15271, 2021. 2

[26] Yu-Chih-Tuan Hu, Jun-Cheng Chen, Bo-Han Kung, Kai-Lung Hua, and Daniel Stanley Tan. Naturalistic physical adversarial patch for object detectors. In *2021 IEEE/CVF International Conference on Computer Vision*, pages 7828–7837, 2021. 2

[27] Rongjie Huang, Mingze Li, Dongchao Yang, Jiatong Shi, Xuankai Chang, Zhenhui Ye, Yuning Wu, Zhiqing Hong, Jiawei Huang, Jinglin Liu, Yi Ren, Yuexian Zou, Zhou Zhao, and Shinji Watanabe. Audiogpt: Understanding and generating speech, music, sound, and talking head. In *Thirty-Eighth AAAI Conference on Artificial Intelligence*, pages 23802–23804, 2024. 2, 3

[28] Wenlong Huang, Fei Xia, Ted Xiao, Harris Chan, Jacky Liang, Pete Florence, Andy Zeng, Jonathan Tompson, Igor Mordatch, Yevgen Chebotar, Pierre Sermanet, Tomas Jackson, Noah Brown, Linda Luu, Sergey Levine, Karol Hausman, and Brian Ichter. Inner monologue: Embodied reasoning through planning with language models. In *Conference on Robot Learning*, pages 1769–1782, 2022. 2

[29] Yihao Huang, Liangru Sun, Qing Guo, Felix Juefei-Xu, Jiayi Zhu, Jincao Feng, Yang Liu, and Geguang Pu. Ala: Naturalness-aware adversarial lightness attack. *arXiv preprint arXiv:2201.06070*, 2022. 2

[30] Brian Ichter, Anthony Brohan, Yevgen Chebotar, Chelsea Finn, Karol Hausman, Alexander Herzog, Daniel Ho, Julian Ibarz, Alex Irpan, Eric Jang, Ryan Julian, Dmitry Kalashnikov, Sergey Levine, Yao Lu, Carolina Parada, Kanishka Rao, Pierre Sermanet, Alexander Toshev, Vincent Vanhoucke, Fei Xia, Ted Xiao, Peng Xu, Mengyuan Yan, Noah Brown, Michael Ahn, Omar Cortes, Nicolas Sievers, Clayton Tan, Sichun Xu, Diego Reyes, Jarek Rettinghouse, Jornell Quiambao, Peter Pastor, Linda Luu, Kuang-Huei Lee, Yuheng Kuang, Sally Jesmonth, Nikhil J. Joshi, Kyle Jeffrey, Rosario Jauregui Ruano, Jasmine Hsu, Keerthana Gopalakrishnan, Byron David, Andy Zeng, and Chu yuan Kelly Fu. Do as I can, not as I say: Grounding language in robotic affordances. In *Conference on Robot Learning*, pages 287–318, 2022. 2

[31] Andrew Ilyas, Shibani Santurkar, Dimitris Tsipras, Logan Engstrom, Brandon Tran, and Aleksander Madry. Adversarial examples are not bugs, they are features. In *Advances in Neural Information Processing Systems 32: Annual Conference on Neural Information Processing Systems*, pages 125–136, 2019. 3, 5

[32] Andrew Ilyas, Shibani Santurkar, Dimitris Tsipras, Logan Engstrom, Brandon Tran, and Aleksander Madry. Adversarial examples are not bugs, they are features. *Advances in neural information processing systems*, 32, 2019. 3

[33] Andrew Ilyas, Shibani Santurkar, Dimitris Tsipras, Logan Engstrom, Brandon Tran, and Aleksander Madry. Adversarial examples are not bugs, they are features. In *Advances in Neural Information Processing Systems*, pages 125–136, 2019. 2

[34] Xiangli Jia, Ying Tong, Hongming Qiao, Man Li, Jiangang Tong, and Baolin Liang. Fast and accurate object detector for autonomous driving based on improved yolov5. *Scientific Reports*, 13, 2023. 2

[35] Glenn Jocher. Ultralytics yolov5, 2020. 3, 6

[36] Zelun Kong, Junfeng Guo, Ang Li, and Cong Liu. Physgan: Generating physical-world-resilient adversarial examples for autonomous driving. In *CVPR*, pages 14254–14263, 2020. 2

[37] Ji Lin, Hongxu Yin, Wei Ping, Pavlo Molchanov, Mohammad Shoeybi, and Song Han. VILA: on pre-training for visual language models. In *IEEE/CVF Conference on Computer Vision and Pattern Recognition*, 2024. 2

[38] Aishan Liu, Xianglong Liu, Jiaxin Fan, Yuqing Ma, Anlan Zhang, Huiyuan Xie, and Dacheng Tao. Perceptual-sensitive gan for generating adversarial patches. In *AAAI*, pages 1028–1035, 2019. 2

[39] Aishan Liu, Jiakai Wang, Xianglong Liu, Bowen Cao, Chongzhi Zhang, and Hang Yu. Bias-based universal adversarial patch attack for automatic check-out. In *ECCV*, pages 395–410. Springer, 2020. 2

[40] Wenyu Lv, Shangliang Xu, Yian Zhao, Guanzhong Wang, Jinman Wei, Cheng Cui, Yuning Du, Qingqing Dang, and Yi Liu. Detrs beat yolos on real-time object detection, 2023. 6

[41] Jiageng Mao, Yuxi Qian, Hang Zhao, and Yue Wang. Gpt-driver: Learning to drive with GPT. *CoRR*, abs/2310.01415, 2023. 2, 3

[42] Jiageng Mao, Shaoshuai Shi, Xiaogang Wang, and Hongsheng Li. 3d object detection for autonomous driving: A comprehensive survey. *International Journal of Computer Vision*, 131(8):1909–1963, 2023. 2

[43] Svetlana Pavlitska, Nico Lambing, and J. Marius Zöllner. Adversarial attacks on traffic sign recognition: A survey. *CoRR*, abs/2307.08278, 2023. 1

[44] Yiran Qin, Enshen Zhou, Qichang Liu, Zhenfei Yin, Lu Sheng, Ruimao Zhang, Yu Qiao, and Jing Shao. MP5: A multi-modal open-ended embodied system in minecraft via active perception. In *IEEE/CVF Conference on Computer Vision and Pattern Recognition+*, pages 16307–16316, 2024. 2

[45] Robin Rombach, Andreas Blattmann, Dominik Lorenz, Patrick Esser, and Björn Ommer. High-resolution image synthesis with latent diffusion models. In *Proceedings of the IEEE/CVF conference on computer vision and pattern recognition*, pages 10684–10695, 2022. 3, 5

[46] Robin Rombach, Andreas Blattmann, Dominik Lorenz, Patrick Esser, and Björn Ommer. High-resolution image synthesis with latent diffusion models. In *Proceedings of the IEEE/CVF conference on computer vision and pattern recognition*, pages 10684–10695, 2022. 6

[47] Takami Sato, Justin Yue, Nanze Chen, Ningfei Wang, and Qi Alfred Chen. Intriguing properties of diffusion models: An empirical study of the natural attack capability in text-to-image generative models. In *IEEE/CVF Conference on*

Computer Vision and Pattern Recognition (CVPR), pages 24635–24644. IEEE, 2024. 1, 2, 3, 6, 5

[48] Murray Shanahan, Kyle McDonell, and Laria Reynolds. Role play with large language models. *Nature*, 623(7987):493–498, 2023. 2

[49] Junjie Shen, Ningfei Wang, Ziwen Wan, Yunpeng Luo, Takami Sato, Zhisheng Hu, Xinyang Zhang, Shengjian Guo, Zhenyu Zhong, Kang Li, Ziming Zhao, Chunming Qiao, and Qi Alfred Chen. Sok: On the semantic AI security in autonomous driving. *CoRR*, abs/2203.05314, 2022. 2

[50] Xiaoqian Shen, Yunyang Xiong, Changsheng Zhao, Lemeng Wu, Jun Chen, Chenchen Zhu, Zechun Liu, Fanyi Xiao, Balakrishnan Varadarajan, Florian Bordes, Zhuang Liu, Hu Xu, Hyunwoo J. Kim, Bilge Soran, Raghuraman Krishnamoorthi, Mohamed Elhoseiny, and Vikas Chandra. Longvu: Spatiotemporal adaptive compression for long video-language understanding. *arXiv:2410.17434*, 2024. 3

[51] Naufal Suryanto, Yongsu Kim, Hyoeun Kang, Harashta Tatimma Larasati, Youngyeo Yun, Thi-Thu-Huong Le, Hunmin Yang, Se-Yoon Oh, and Howon Kim. Dta: Physical camouflage attacks using differentiable transformation network. In *CVPR*, pages 15305–15314, 2022. 2

[52] Jia Tan, Nan Ji, Haidong Xie, and Xueshuang Xiang. Legitimate adversarial patches: Evading human eyes and detection models in the physical world. In *ACMMM*, pages 5307–5315, 2021. 2

[53] Simen Thys, Wiebe Van Ranst, and Toon Goedemé. Fooling automated surveillance cameras: adversarial patches to attack person detection. In *Proceedings of the IEEE/CVF conference on computer vision and pattern recognition workshops*, pages 0–0, 2019. 2

[54] Ao Wang, Hui Chen, Lihao Liu, Kai Chen, Zijia Lin, Jungong Han, and Guiguang Ding. Yolov10: Real-time end-to-end object detection. *arXiv preprint arXiv:2405.14458*, 2024. 6

[55] Guanzhi Wang, Yuqi Xie, Yunfan Jiang, Ajay Mandlekar, Chaowei Xiao, Yuke Zhu, Linxi Fan, and Anima Anandkumar. Voyager: An open-ended embodied agent with large language models. *Trans. Mach. Learn. Res.*, 2024. 2

[56] Jiakai Wang, Aishan Liu, Xiao Bai, and Xianglong Liu. Universal adversarial patch attack for automatic checkout using perceptual and attentional bias. *IEEE Transactions on Image Processing*, 31:598–611, 2021. 2

[57] Jiakai Wang, Aishan Liu, Zixin Yin, Shunchang Liu, Shiyu Tang, and Xianglong Liu. Dual attention suppression attack: Generate adversarial camouflage in physical world. In *CVPR*, pages 8565–8574, 2021. 2

[58] Ningfei Wang, Yunpeng Luo, Takami Sato, Kaidi Xu, and Qi Alfred Chen. Does physical adversarial example really matter to autonomous driving? towards system-level effect of adversarial object evasion attack. In *IEEE/CVF International Conference on Computer Vision*, pages 4389–4400, 2023. 2

[59] XuDong Wang, Shaolun Zhang, Shufan Li, Konstantinos Kallidromitis, Kehan Li, Yusuke Kato, Kazuki Kozuka, and Trevor Darrell. Segllm: Multi-round reasoning segmentation. *arXiv:2410.18923*, 2024. 3

[60] Hui Wei, Hao Tang, Xuemei Jia, Zhixiang Wang, Hanxun Yu, Zhubo Li, Shin'ichi Satoh, Luc Van Gool, and Zheng Wang. Physical adversarial attack meets computer vision: A decade survey. *IEEE Transactions on Pattern Analysis and Machine Intelligence*, 46(12):9797–9817, 2024. 1

[61] Jason Wei, Xuezhi Wang, Dale Schuurmans, Maarten Bosma, Brian Ichter, Fei Xia, Ed H. Chi, Quoc V. Le, and Denny Zhou. Chain-of-thought prompting elicits reasoning in large language models. In *Advances in Neural Information Processing Systems*, 2022. 2

[62] Xingxing Wei, Ying Guo, Jie Yu, and Bo Zhang. Simultaneously optimizing perturbations and positions for black-box adversarial patch attacks. *IEEE Transactions on Pattern Analysis and Machine Intelligence*, 2022. 2

[63] Xingxing Wei, Yao Huang, Yitong Sun, and Jie Yu. Unified adversarial patch for visible-infrared cross-modal attacks in the physical world. *IEEE Transactions on Pattern Analysis and Machine Intelligence*, 2023. 2

[64] Yun Xing, Qing Guo, Xiaofeng Cao, Ivor W. Tsang, and Lei Ma. Metarepair: Learning to repair deep neural networks from repairing experiences. In *Proceedings of the 32nd ACM International Conference on Multimedia*, pages 1781–1790, 2024. 2

[65] Kaidi Xu, Gaoyuan Zhang, Sijia Liu, Quanfu Fan, Mengshu Sun, Hongge Chen, Pin-Yu Chen, Yanzhi Wang, and Xue Lin. Adversarial t-shirt! evading person detectors in a physical world. In *ECCV*, pages 665–681. Springer, 2020. 2

[66] Haotian Xue, Alexandre Araujo, Bin Hu, and Yongxin Chen. Diffusion-based adversarial sample generation for improved stealthiness and controllability. In *Advances in Neural Information Processing Systems*, 2023. 2

[67] Darren Yu Yang, Jay Xiong, Xincheng Li, Xu Yan, John Raiti, Yuntao Wang, HuaQiang Wu, and Zhenyu Zhong. Building towards" invisible cloak": Robust physical adversarial attack on yolo object detector. In *2018 9th IEEE Annual Ubiquitous Computing, Electronics & Mobile Communication Conference (UEMCON)*, pages 368–374. IEEE, 2018. 2

[68] Jianwei Yang, Hao Zhang, Feng Li, Xueyan Zou, Chunyuan Li, and Jianfeng Gao. Set-of-mark prompting unleashes extraordinary visual grounding in gpt-4v, 2023. 4, 5

[69] Ling Yang, Zhaochen Yu, Chenlin Meng, Minkai Xu, Stefano Ermon, and Bin Cui. Mastering text-to-image diffusion: Recaptioning, planning, and generating with multimodal llms. In *Forty-first International Conference on Machine Learning*, 2024. 2, 3

[70] Hao Zhang, Hongyang Li, Feng Li, Tianhe Ren, Xueyan Zou, Shilong Liu, Shijia Huang, Jianfeng Gao, Leizhang, Chunyuan Li, and Jainwei Yang. Llava-grounding: Grounded visual chat with large multimodal models. In *Computer Vision - ECCV*, pages 19–35, 2024. 2

[71] Shibo Zhang, Yushi Cheng, Wenjun Zhu, Xiaoyu Ji, and Wenyuan Xu. {CAPatch}: Physical adversarial patch against image captioning systems. In *32nd USENIX Security Symposium (USENIX Security 23)*, pages 679–696, 2023. 2

[72] Yang Zhang, Hassan Foroosh, Philip David, and Boqing Gong. CAMOU: learning physical vehicle camouflages to adversarially attack detectors in the wild. In *7th International Conference on Learning Representations (ICLR)*, 2019. 2

[73] Zhuosheng Zhang and Aston Zhang. You only look at screens: Multimodal chain-of-action agents. In *Findings of the Association for Computational Linguistics*, pages 3132–3149. Association for Computational Linguistics, 2024. 2

[74] Jingyuan Zhao, Wenyi Zhao, Bo Deng, Zhenghong Wang, Feng Zhang, Wenxiang Zheng, Wanke Cao, Jinrui Nan, Yubo Lian, and Andrew F. Burke. Autonomous driving system: A comprehensive survey. *Expert Syst. Appl.*, 242, 2024. 2

[75] Yiqi Zhong, Xianming Liu, Deming Zhai, Junjun Jiang, and Xiangyang Ji. Shadows can be dangerous: Stealthy and effective physical-world adversarial attack by natural phenomenon. In *CVPR*, pages 15345–15354, 2022. 2

MAGIC: Mastering Physical Adversarial Generation in Context through Collaborative LLM Agents

Supplementary Material

1. Experimental Environment

We employ ChatGPT (gpt-4o-2024-08-06) as the LLM backend for all the agents in our design. All the experiments are conducted via a server with AMD EPYC 9554 64-core Processor and an NVIDIA L40 GPU, running Ubuntu 22.04.

2. Implementation Details

We give out the technical details for implementing the proposed MAGIC framework. Specifically, there are two main aspects: ❶ the setting adopted for text-to-image (T2I) model, ❷ the parameters for object detectors and ❸ the set-of-mark prompting hyper-parameters.

T2I Model. We apply Stable Diffusion v2 as the text-to-image generation backend, where the checkpoint is released by StabilityAI on huggingface [1]. Following the official example, we set the sampling scheduler as EulerDiscreteScheduler. As for the hyper-parameters, we set guidance_scale $= 7.5$ and the negative_prompt as "deformed, distorted, disfigured, poorly drawn, bad anatomy, wrong anatomy, extra limb, missing limb, floating limbs, mutated hands and fingers, disconnected limbs, mutation, mutated, ugly, disgusting, blurry, amputation, NSFW". All other parameters are set to default.

Object Detector. For the evaluated object detectors, we directly invoke API from ultralytics [2] where the default hyper-parameter setting is adopted.

SoM Prompting. We adopt the official set-of-mark (SoM) implementation [3] through our experiments. The only changes to the parameters is that we use slider $= 1.8$ while all the other parameters are set to default

3. The Pre-defined Goals & Rules

As the supplements for Instruction $\mathcal{X}_{\mathrm{D}}$ and $\mathcal{X}_{\mathrm{D}}$, below we first show the details of the definition of attack and deployment goal, and the rules of how to realize attack is detailed in the next page due to the large size of the text.

Definition of Attack & Deployment Goal

We focus on the task of attacking an object detector with a visual patch in the real world, where the visual patch is an image generated by a text-to-image model based on a given text prompt and 'in the real world' means the effectiveness of the visual patch is evaluated after deploying it into a real-world environment. All the procedures for generating, deploying and evaluating the visual patch are detailed in the provided PIPELINE.

[1] https://huggingface.co/stabilityai/stable-diffusion-2

[2] https://github.com/ultralytics/ultralytics

[3] https://github.com/microsoft/SoM

Following the PIPELINE, let's specify a category with name 'xxx' as an example. We define an effective visual patch is an image that 1) can successfully attack the object detector by itself only, and 2) can successfully attack the object detector after it is deployed into an environment. The word 'attack' here means that 1) the object detector recognizes the visual patch as an instance of category 'xxx' with high confidence, but 2) human observers think the visual patch is just an abstract art which does not belongs to any specific category. Note that the high confidence refers to the confidence score of a detection result is higher than the provided CONF_THRESHOLD. In summary, the ultimate goal of the PIPELINE is to obtain an effective visual patch as defined above.

- **PIPELINE:** The pipeline consists of three modules: the text-to-image generation module, the visual patch deployment module and the object detection module. For a round of generation, deployment and evaluation, the data and their flow are detailed as follows:
  (Specify an object category, e.g., 'xxx', before all the procedures.)
  1) the process begins with the input text prompt with category 'xxx' as the grammatical subject.
  2) then the text-to-image model generates a visual patch with the input text prompt, where the goal is to create an image that composed of all the objects and features described in the text prompt;
  3) a real-world image which represents the real-world environment is given;
  4) then a visual patch deployment module conduct the deployment process,
  a. first list all the regions, poles and beams in the given environment image that can be utilized to either paint or hang the visual patch
  b. select one region, pole or beam from the list that can keep the visual patch's effectiveness and make it coherent with the environment;
  5) finally, the object detector conduct evaluation for both the visual patch itself and the environment image with the patch deployed;
  6) the detection results give out the confidence of recognizing the visual patch as specific category.
- **CONF_THRESHOLD:** 0.80

4. More Experimental Results

4.1. Statistical Results of Naturalness

In section Sec. 5.2, we visually compare the naturalness of our MAGIC patches. As the naturalness is measured by the LLM $\mathcal{E}$ with the instruction γ which gives out a naturalness score for each deployed patch. Here, we tabulate the average score results over the evaluated 6 environments. As we can see from Tab. 4, our MAGIC patches consistently get higher average naturalness score over all the environments.

Table 4. The average naturalness score results over 6 environments.

	Env①	Env②	Env③	Env④	Env⑤	Env⑥
NDDA Rand	0.22	0.40	0.37	0.20	0.20	0.33
NDDA *w/* DAgent	0.50	0.70	0.77	0.60	0.70	0.70
MAGIC (ours)	**0.91**	**0.89**	**0.99**	**0.97**	**0.94**	**0.93**

Rules to Realize Attack

Essentially, the effectiveness of an visual patch derives from its deceptive appearance which is solely controlled by the text prompt during the text-to-image generation. As a result, an effective visual patch can be obtained by intentionally modifying the descriptive text prompt. Given the fact that the detector and human recognize an object as its category based on the robust features, altering the description of robust features while keep using the original category name in the text prompt is the practical method to generate an effective visual patch. The robust features of an object and examples for altering the description are explained in the provided ROBUST_FEATURE.

- **ROBUST_FEATURE:** In general, the robust features of an object refers to the characteristics or attributes that remain consistent and identifiable across various conditions, environments, and perspectives. They help in accurately identifying and classifying objects despite changes such as lighting, orientation, scale, or noise. Robust features should maintain their distinctiveness and reliability under transformations such as:
  1) Translation: The object can be moved or positioned differently in the frame.
  2) Rotation: The object can be rotated at various angles.
  3) Scale: The object can appear larger or smaller.
  4) Illumination: Lighting conditions can change, affecting the object's appearance.
  5) Occlusion: Part of the object might be obstructed or hidden.
  6) Noise: Data might be corrupted by external disturbances.

  Take the robust features of a stop sign as example, they contains:
  1) Octagonal Shape: Stop signs are standardized as octagons;
  2) Red Color: The background is red, which is a typical color for stop signs to signify the need to stop;
  3) White Text: The word "STOP" is in white, which contrasts well against the red background, making it easily readable;
  4) Universal Recognition: The combination of these features is commonly used worldwide to indicate a stop sign;
  5) High Contrast: The red and white color scheme provides high contrast for easy visibility;
  6) Simplicity: Minimalist design for quick recognition and action.

  Here are some examples of altering the description of robust features while keep using the original category name in a text prompt:
  The original text prompt: "A stop sign."
  Example 1: "A yellow triangle stop sign."
  Example 2: "A blue square stop sign with 'HELLO' on it."
  Example 3: "A triangle stop sign with 'WORLD' on it and checkerboard paint on it."
  The original text prompt: "A traffic light."
  Example 1: "A blue, white, pink traffic light."
  Example 2: "A heart shape white, gray, orange traffic light."
  Example 3: "A blue, white, pink traffic light with polka dots.""

4.2. Robustness to Real-world Factors

As mentioned in Sec. 4.5, our MAGIC performs robust to common digital-to-physical (D2P) factors like printing color shift and viewing angle change, which are well-know to degrade the performance. We conduct experiments to prove our MAGIC superiority as illustrated in Fig. 1 and Fig. 2.

Digital-to-physical Transferability. To verify the transferability with fairness, we select one typical effective patch for each type of text prompt in NDDA, then we deploy them into two environments with location variations. For our proposed MAGIC, we directly feed the environmental image into the pipeline to get the patches. The deployment process for both NDDA and MAGIC patches are kept the same.

Results. As illustrated in Fig. 1, we first notice that ❶ **different environments and deployment placements affect the D2P transferability a lot**. NDDA patch's attack performance degrades significantly by deploying the patches in different environments (Fig. 1 columns in red boundbox) or with changed placement (Fig. 1 columns in green boundbox). ❷ Then, we observe that ❶ **NDDA's robust feature removal greatly deteriorates D2P transferability.** All variants of NDDA patches (Fig. 1 columns) show significant performance drop after the patches are deployed into the real world. However, as our MAGIC results shown Fig. 1, ❸ **our LLM-based framework enhances D2P transferability**. The proposed MAGIC adaptively optimize the patch generation and placement with environment understanding through iterative agent planning which resulting in enhanced D2P transferability with consistently high confidence across environments. Such strong performance proves our MAGIC's

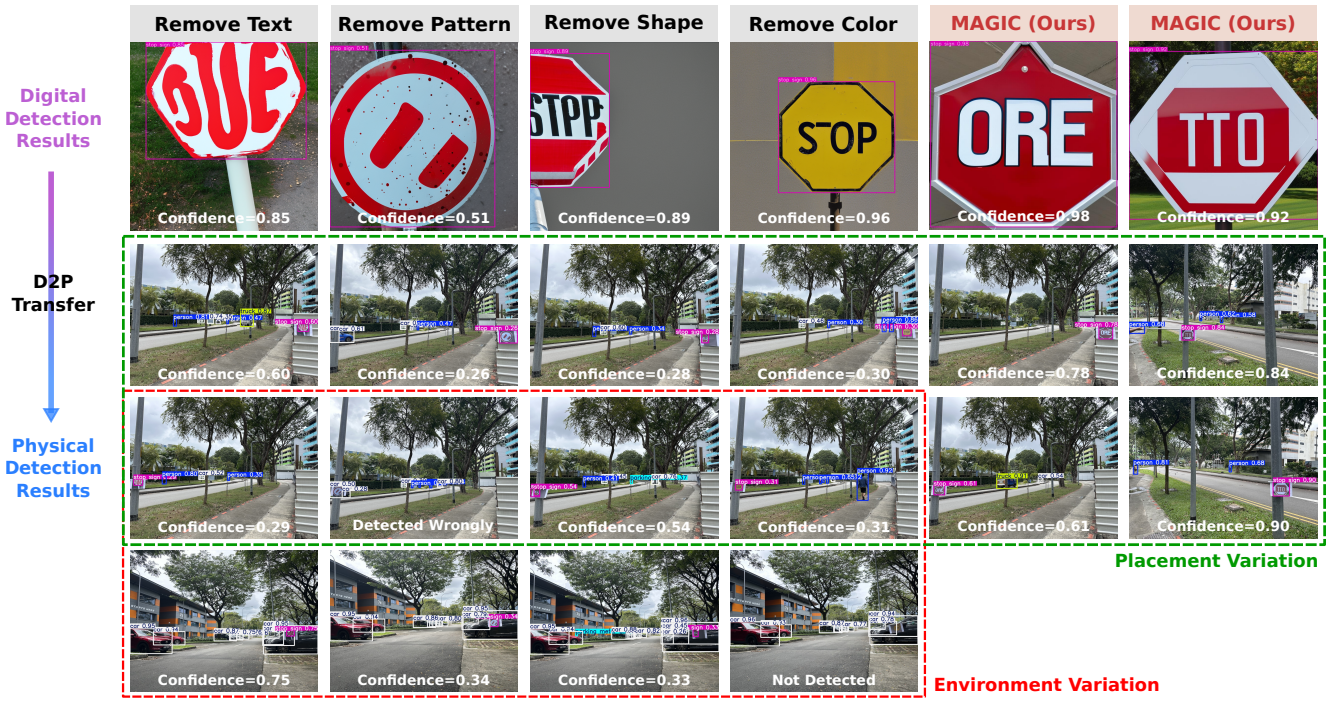


Figure 1. Digital-to-physical transfer visualization results of NDDA and MAGIC.

capability of performing robust to real-world influences.

Robustness of Viewing Angle & Distance To demonstrate the robustness of our MAGIC to viewing angle and distance, we set three levels of patch size (*i.e.*, 128, 160, 192 pixels) to simulate the viewing distance and three different angle (*i.e.*, 15, 30 and 45 degrees). As shown in Fig. 2, we deploy of our MAGIC patch into the bus stop scene with the specified angle and size setup. Furthermore, we plot the cross performance for more viewing angles against the three distance.

Results. As we can see from the radar plot in Sec. 3.2, our MAGIC patch consistently performs great across different viewing angles and distances. Such performance can also be observed form the illustration of physical evaluation results. Even there exists a degradation of detection confidence, our MAGIC patch still successfully mislead the detector to detect the patch as a stop sign with high confidence (> 0.5).

4.3. Physical Experiments

To support the physical deployment effectiveness of our proposed MAGIC, we conduct more physical experiments to support the superior performance of our proposed MAGIC framework. As shown in Fig. 3 and Fig. 4, we apply MAGIC to generate and deploy for three more different environments. Following the same strategy, we first test whether MAGIC can consistently generate effective patch for multiple round of execution given an environment. The results is illustrated in Fig. 3 and we can observe that all three different generated patches are effective to attack the three detectors. For the

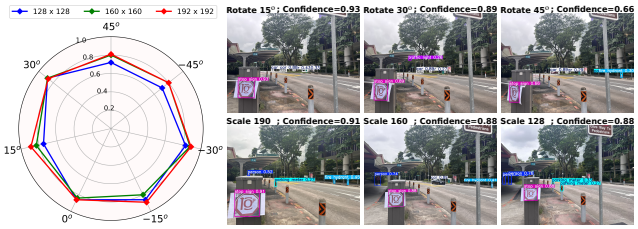


Figure 2. Viewing distance and angle results for MAGIC patches.

distinct environment attacking, the physical cases shown in Fig. 4 further support our conclusion that our MAGIC is full of power for attacking the object detection system in the real-world scenarios.

5. Ethical Consideration

Our work highlights the ethical responsibility associated with adversarial research. Without proper safeguards, such techniques could be misused to exploit critical systems, underscoring the need for responsible disclosure and research collaboration to mitigate risks. As discussed in [47], mitigation of attacks in this line of work can involve OCR-based detection in the cases of stop signs, or "robustified" training [31]. However, no generic defense strategies have been reported, so further mitigation research efforts would be much appreciated. Ultimately, our research aims to contribute to the development of secure, trustworthy autonomous driving systems and implemented strict safeguards: ❶ attacks are not visible to AV on public roads during the physical experiments; ❷ access control to verified researchers; ❷ all the

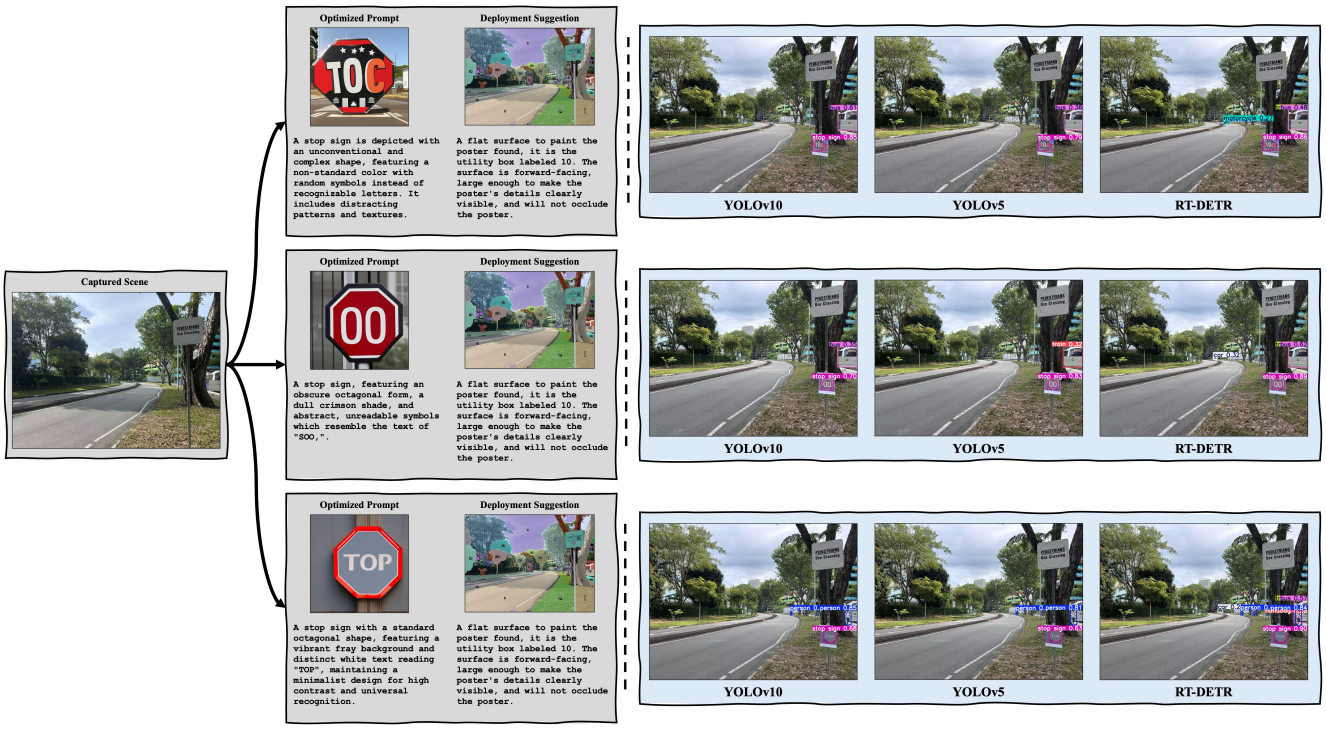


Figure 3. Illustration of the physical attacking cases and the corresponding object detector evaluation results, where our MAGIC can generate several different effective patches for given specific environment. The gray region enclosed the patch and the deployment suggestion generated by our MAGIC framework, while the blue region enclosed the results of evaluation with the three object detectors. Please zoom in for better visualization.

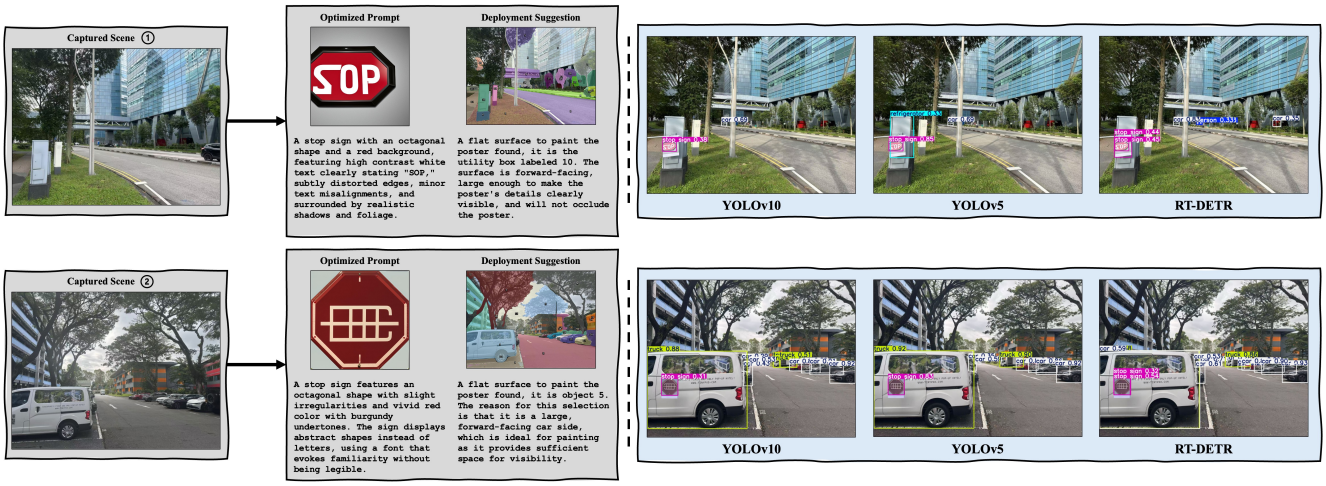


Figure 4. Illustration of the physical attacking cases and the corresponding object detector evaluation results. Scene ❶: A real-world road with heavy traffics. Scene ❷: A parking area with car in and out. The gray region enclosed the patch and the deployment suggestion generated by our MAGIC framework, while the blue region enclosed the results of evaluation with the three object detectors. Please zoom in for better visualization.

generated patches are under traceable tools monitoring. This controlled approach enables advancing AI security research while preventing misuse.

6. Limitations

The scope of our work is focused on designing physical adversarial attack in traffic scenarios via LLM agents. ❶ Nevertheless, the current environments primarily serve as proofs of concept under standard conditions, rather than encompassing a broader range of factors such as varying weathers, daylight and nighttime conditions, or noisy camera inputs. ❷ Furthermore, our framework has not yet considered seamless blending between natural adversarial patches and its environment in their digital implementations. We believe

that extending this work to include comprehensive analyses of appearance blending using diffusion techniques could significantly enhance its applicability, as well as bringing discussions on the attacks' broader impacts. In general, our study made the initial step to investigate the natural diffusion generation attack in physical world, but real-world situations are complicated which requires more generalizable attacks.

7. Broader Impact

Understanding vulnerabilities in traffic systems can help improve the safety and resilience of autonomous vehicles. In fact, by rigorously testing adversarial robustness across diverse real-world conditions, we can identify potential risks and develop countermeasures to ensure that these systems function well in dynamic environments. Meanwhile, our work also highlights the ethical responsibility associated with adversarial research. Without proper safeguards, such techniques could be misused to exploit critical systems, underscoring the need for responsible disclosure and research collaboration to mitigate risks. As discussed in [47], mitigation of attacks in this line of work can involve OCR-based detection in the cases of stop signs, or "robustified" training [31]. However, no generic defense strategies have been reported, so further research efforts for mitigation of the attacks would be much appreciated. Ultimately, our research aims to contribute to the development of secure, trustworthy autonomous driving systems.

8. Future Work

Our future work aims to explore larger-scale attacks to evaluate adversarial vulnerabilities across broader traffic systems, including segmentation and depth estimation tasks critical for autonomous navigation. Furthermore, integrating advanced blending techniques, such as diffusion models, could enhance the realism and effectiveness of natural adversarial patches, enabling more comprehensive testing under diverse environmental conditions. Importantly, as also suggested by the lack of investigation for robust defenses, we aim to develop robust defense mechanisms to counter natural diffusion attacks both digitally and physically, would be essential for ensuring safety and resilience in real-world applications.